Egypt. J. Chem. **Vol. 68,** SI: Z. M. Nofal, pp. 145 - 160 (2025)

Egyptian Journal of Chemistry

http://ejchem.journals.ekb.eg/

The Potential Application of Antifungal Chitosan Nanoparticles against *Fusarium oxysporum* Fungus of Cumin

Shimaa A. Salem[1,2*]; Ahmed S. H.[1]; Ahmed O. K.[1]; Sherif, S.[2,3]; Elwan, S. E.[4]

[1] *Biochemistry Department, Faculty of Agriculture, Cairo University*

[2]*Medicinal and Aromatic Plants Research Department, Horticulture Research Institute, Agricultural Research Centre, Cairo, Egypt.*

[3]*Tissue Culture Lab., Hort. Res. Institute, A. R. C., Egypt.*

[4]*Fungi Diseases Dept. Plant Pathology Research Institute, Agricultural Research Center, Egypt.*

Abstract

Fusarium wilt, a disease affecting cumin *(Cuminum cyminum L.*) and caused by *Fusarium oxysporum* f. sp. *cumini*, has been detected in both early and mature growth stages across major cumin-producing areas in southern Egypt. The present study focuses on analyzing specific phytochemical components, fabricating chitosan nanoparticles (CNPs) using essential oil extracted from *C. cyminum*(CO) and guava leaf extract (GE), and examining the influence of different natural stabilizing agents (bio-reducers) on nanoparticle formation efficiency. Furthermore, the antifungal potential of these nanoparticles against *F. oxysporum*, along with their cytotoxic impact on human cells, was evaluated. The CNPs were synthesized under various conditions using an aqueous chitosan solution and bio-reductants (CO and GE), and were characterized through dynamic light scattering (DLS), zeta potential measurement, transmission electron microscopy (TEM), Fourier-transform infrared spectroscopy (FTIR), and X-ray diffraction (XRD). Antifungal activity was tested both *in vitro* and *in vivo*, with additional assessment of morphological and chemical parameters in living plants. Results indicated rapid nanoparticle formation, producing mostly spherical particles ranging from 9.71 to 21.30 nm for CO-based CNPs, and 1.02 to 29.4 nm for those synthesized with GE. Notably, the GE-CNPs exhibited potent antifungal activity against *F. oxysporum*.

Keywords; *Cuminum cyminum* L.; *Fusarium* wilt; *Fusarium oxysporum*; chitosan nanoparticles; guava leaf extract; antifungal activity; cytotoxicity.

1. Introduction

In recent years, medicinal and aromatic plants have gained increasing attention due to their effectiveness, natural origin, minimal adverse effects, and ease of accessibility. This is primarily attributed to their richness in bioactive compounds that exhibit potent antimicrobial and antifungal effects [1]. Plants like cumin and guava, for instance, serve dual purposes — as culinary ingredients and as sources of therapeutic agents [2]and [1]. Traditionally, guava leaves have been used in folk medicine to alleviate conditions such as diarrhea, cough, and fever [1]. *Cuminum cyminum* is a herbaceous plant known for its branched stems, brownish seeds, and aromatic, sweet-spicy flavor [2]. It is commonly used in various cuisines across South Asia, North Africa, and Latin America [3]. Apart from its culinary applications, cumin possesses medicinal benefits such as anti-inflammatory, digestive, and antimicrobial effects [2] and [4].

According to [5], a significant proportion of crop losses—estimated between 20% and 40%—are attributed to factors such as poor soil health, nutritional deficiencies, pest infestations, and microbial infections. Among microbial diseases, fungal infections account for nearly 70–80% of the total. One of the most harmful soil-borne fungi affecting cumin crops is *Fusarium oxysporum*, particularly its special form f. sp. *cumini*, which attacks cumin plants through root invasion at all growth stages [6]and [7]. This pathogen causes wilt and stunted growth, often accompanied by vascular browning, which can result in total crop loss [4]. Recent studies have shown that climate change—through rising temperatures, altered precipitation patterns, increased humidity, and longer growing seasons—can increase crop susceptibility to fungal pathogens such as *Fusarium*, creating more favourable conditions for their growth, reproduction, and geographic spread [8].Due to its persistent nature in soil, effective and sustainable management strategies are essential [9].

*Corresponding author e-mail: shimaaabdalla194@yahoo.com.; (**Shimaa Abd-Allah Salem**).

Received date 16 July 2025; Revised date 14 August 2025; Accepted date 08 September 2025

DOI: 10.21608/EJCHEM.2025.388894.12056

Conventional methods such as soil fumigation, crop rotation, seed treatments, and cultivating resistant varieties have been used to combat *Fusarium*-related diseases [10] and [11]. Synthetic fungicides, though effective and fast-acting [12] and [13], pose serious concerns for human health and the environment. These risks are often exacerbated by excessive or improper use due to limited farmer awareness [14]. Chemical residues can degrade soil quality, pollute the environment, and accumulate in plant tissues [10], [11] and [12]. Additionally, these treatments may not be economically feasible for many growers [10]. Alternatively, bio-fungicides derived from natural sources, such as essential oils, plant extracts, and beneficial microbes, offer safer, cost-effective, and eco-friendly solutions for soil pathogen management [15] and [16]. In this context, nanotechnology emerges as a promising field offering both antifungal activity and growth-promoting properties [17]. Nanoparticles, which include metal oxides, non-metals, and metalloids, are recognized for their nanoscale dimensions, increased reactivity, and large surface area [18]. For instance, [17] reported that zinc oxide nanoparticles (ZnO-NPs) could significantly reduce wilt severity in *Solanum melongena* L. by up to 75%. However, the chemical synthesis of such particles often involves high costs, extended processing times, and potential genotoxicity. Thus, green synthesis has become increasingly popular due to its environmentally friendly, non-toxic, sustainable, and affordable nature [19] and [20].

Among various green-synthesized nanomaterials, chitosan-based nanoparticles have shown significant promise. Chitosan, derived from chitin through deacetylation, makes up 20–30% of crustacean shell waste [20] and [21]. Its applications span environmental, agricultural, and medical fields owing to its multifaceted biological properties such as antimicrobial, anti-inflammatory, antioxidant, anticancer, and antidiabetic effects [20].

The current study aims to synthesize chitosan-based nanoparticles using natural extracts from cumin oil and guava leaves to control wilt disease in cumin plants caused by *Fusarium oxysporum* f. sp. *cumini*. The research also investigates the phytochemical properties of the extracts and evaluates the antifungal potential of the synthesized nanoparticles both under laboratory and greenhouse conditions.

2. Materials and Methods

2.1 Plant Materials
Seeds of *Cuminum cyminum* L. and leaves of *Psidiumguajava*L.were sourced from the Department of Medicinal and Aromatic Plants, Horticulture Research Institute (HRI), Agricultural Research Center (ARC), Egypt.

2.2 Fungal Strain
The pathogenic fungus *Fusarium oxysporum* (Accession no. OR734798) was obtained from the Plant Pathology Research Institute, ARC, Egypt.

2.3 Chemicals
Low molecular weight chitosan (50–190 kDa, 75–85% deacetylation) was purchased from Sigma-Aldrich. The fungicide Rezolex® was obtained from HRI, ARC.

2.4 Growth Media
Potato Dextrose Agar (PDA) and corn meal medium were acquired from Sigma-Aldrich.

2.5 Cumin Essential Oil (CO)
Cumin oil was provided by the Horticulture Research Institute, Agricultural Research Center.

2.6 Preparation of Guava Leaf Extract (GE)
Dried guava leaves (25 g) were powdered and boiled in 100 mL sterile distilled water for 30 minutes to deactivate enzymes. The extract was filtered using Whatman No. 1 filter paper and used for further experiments.

2.7 Pathogen and Antagonist Isolation
Fungal isolates were obtained from infected cumin root and stem tissues, as well as surrounding soil, collected from Giza Governorate. Surface-sterilized tissues were placed on PDA supplemented with chloramphenicol and incubated at 25 ± 2 °C for 5–7 days. Soil samples were serially diluted, plated on PDA, and incubated for 5 days. Fungal colonies were sub-cultured and preserved on PDA slants.

2.8 GC-MS Analysis of Cumin Oil (CO)
Cumin essential oil was subjected to gas chromatography–mass spectrometry (GC-MS) to identify volatile components.

2.9 Synthesis of GE-Loaded Chitosan Nanoparticles (CNPs)
GE-loaded CNPs were synthesized by ionic gelation. Chitosan (0.3% w/v) was dissolved in 1% acetic acid, centrifuged, and

filtered. The pH was adjusted to 4.6–4.8. GE (0.5% w/v) was mixed with 0.25% TPP solution, then added dropwise to 10 mL of chitosan solution under stirring (800 rpm). The mixture was stirred for 1 hour, centrifuged at 9000×g, and keep cooling after washing.

2.10 Synthesis of CO-Loaded Chitosan Nanoparticles
Chitosan (1% w/v) was dissolved in 1% acetic acid, centrifuged, and filtered. Tween 80 (80 mg) was added, and the pH adjusted to 4.2. The mixture was stirred at 50 ℃ for 90 minutes. CO was added (1:0.25 chitosan/oil ratio) under ultrasonication waves in an ice bath. TPP was added to initiate gelation. After stirring for 40 minutes, particles were harvested, washed, and keep cooling for used.

2.11 Nanoparticle Characterization

Particle Size & Zeta Potential: Measured by dynamic light scattering (DLS) using a Malvern Zetasizer Nano-ZS90.

FTIR Spectroscopy: Structural analysis was performed using FTIR over 400–4000 cm^{-1}.

XRD Analysis: Crystallinity was assessed over a 2θ range of 5°–60° using a RigakuMiniFlex 600 diffractometer.

TEM Analysis: Morphology and size were evaluated using transmission electron microscopy (JEOL JEM–2100, 200 kV).

2.12 Antifungal Activity

2.12.1 *In Vitro* Assay

The antifungal efficacy of CNPs was assessed using the disc diffusion method. Filter paper discs impregnated with various concentrations (0–500 ppm) of GE- or CO-loaded CNPs were placed on PDA plates inoculated with *F. oxysporum*. Plates were incubated at 25 ℃ for 7 days, and mycelial inhibition was measured at 48, 96, and 168 hours.

2.12.2 *In Vivo* Assay
Plastic pots (15×20 cm) were filled with 1 kg of sterilized sandy soil. Ten cumin seeds were sown in each pot. The soil was infested with *F. oxysporum* grown on corn meal media (CMM) and PDA. Treatments included:

Untreated control

Infected control

Infected + Rezolex (0.2%)

Infected + GE-CNPs (500 ppm)

Infected + GE-CNPs (1000 ppm)

Infected + GE-CNPs (1500 ppm)
Experiments were arranged in a randomized block design with three replicates under greenhouse conditions (20 ± 2 °C, 75 ± 2% RH, 14/10 h light/dark). After 35 days, plants were harvested, and morphological and dry weight measurements were recorded.

3. Morphological Evaluation and Growth Parameters

Several germination and seedling growth metrics were assessed. Germination percentage (GP%) was calculated as:

GP% = (Number of germinated seeds / Total seeds) × 100[11].

Shoot length (SL), root length (RL), and the number of leaves were measured for six seedlings per treatment using a measuring tape. The shoot-to-root length ratio was then derived for each treatment.

2.14. Chemical Analysis

2.14.1. Total Soluble Phenolic Content

Phenolic content was determined using the method described by [22].

2.14.2. Total Soluble Flavonoid Content

Flavonoid content was quantified according to the protocol by [23].

2.14.3. Total Antioxidant Activity (%)

The antioxidant capacity was assessed using the DPPH radical scavenging method following [24]. Absorbance was measured at 517 nm, and antioxidant activity was calculated as:

Antioxidant activity (%) = [(Control OD − Sample OD) / Control OD] × 100

2.14.4. Essential Oil Yield (%)

Essential oil (EO) was extracted from 800 g of dried plant material using hydro-distillation with a Clevenger apparatus for 3 hours [25]. EO was dried with anhydrous sodium sulfate and stored at 4 °C. The oil yield was expressed as weight percentage (w/w) and yield per 100 plants.

2.14.5. GC-MS Analysis

EO composition was analyzed using a TRACE GC Ultra Gas Chromatograph (THERMO Scientific, USA) coupled to a THERMO ISQ Mass Spectrometer. The separation was performed on a TR-5MS capillary column using helium as the carrier gas. Identification of compounds was based on retention time and spectral comparison with mass spectral libraries [26] and [27].

2.15. Cytotoxic and Cellular Assays

2.15.1. Cell Culture

A549 (NSCLC) and Vero cell lines were cultured in RPMI-1981 medium with 10% fetal bovine serum and standard supplements. Cells were maintained at 37 °C in a humidified 5% CO_2 atmosphere and passaged upon reaching 75% confluence.

2.15.2. Cytotoxicity Assay (MTT)

The viability of Vero cells treated with cumin oil obtained from (a) oil obtained from Rezolex ® treated plants; (b) oil obtained from untreated plants (negative control); (c) oil obtained from plants treated with CNPs+ GE at 1500 pm (d) oil obtained from infected plants (positive control) was assessed using the MTT assay, which measures mitochondrial dehydrogenase activity. Formazan crystals formed were dissolved in acidified isopropanol, and absorbance was recorded at 570 nm. Cell viability was calculated as:

Relative viability (%) = (Absorbance of treated cells / Absorbance of control cells) × 100

IC_{50} values were estimated using linear regression [28].

2.15.3. Cell Proliferation Assay

Cells (10^4–10^6) were seeded into 96-well plates and treated with rutin concentrations ranging from 18.75 to 500 µg/mL. After 24 h incubation, viability was assessed as described, and absorbance measured at 570 nm using an ELISA plate reader [29].

2.15.4. Statistical Analysis

Data were analyzed using a completely randomized design (CRD). Means were compared using LSD at 5% significance level, following the method of [30].

3. Results and discussion

3.1. Nanoparticle Characterization

3.1.1. FTIR Analysis

Fourier-transform infrared (FTIR) spectroscopy confirmed the formation of chitosan nanoparticles (CNPs) and their interaction with guava extract and cumin oil. Chitosan showed characteristic peaks at 1643, 1005, and 3450 cm^{-1} corresponding to amide, glucosidic, and amine groups, respectively (Fig. 1).

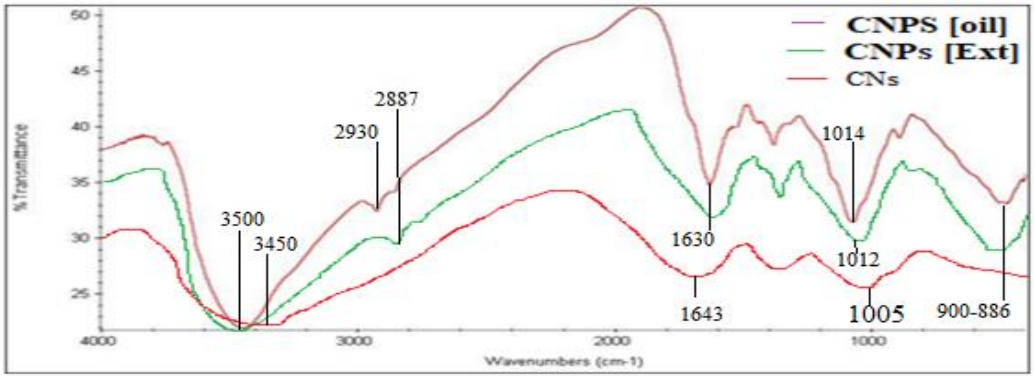

Fig. 1. FTIR analysis of chitosan, CO loaded CNPs and GE loaded CNPs.

In CNPs loaded with extracts, shifts to lower wavenumbers (e.g., 1612 and 1630 cm^{-1}) indicated interactions between chitosan's functional groups and bioactive compounds, suggesting increased hydrogen bonding and cross-linking [31]. Additional peaks between 3500–3300 cm^{-1} (O–H stretching) and at 1531, 1012, and 886 cm^{-1} confirmed structural modifications and nanoparticle formation.

3.1.2.Dynamic Light Scattering (DLS) Analysis

The particle size distribution of the chitosan nanoparticles (CNPs) was analyzed using dynamic light scattering (DLS), as shown in **Figure 2**. The results revealed that CNPs loaded with cumin essential oil and guava leaf extract exhibited diameters ranging from approximately **98.7 to 110 nm**, with a narrow size distribution and a stable polydispersity index. This size range reflects chemical modifications occurring during nanoparticle formation from the chitosan biopolymer.

The mean hydrodynamic diameter recorded was **259.4 nm**, which is notably larger than values observed by transmission electron microscopy (TEM). This discrepancy is attributed to the swelling behavior of the chitosan hydrogel in aqueous environments during DLS analysis, in contrast to the shrinkage in dry-state TEM imaging [32].

Prior studies have highlighted the efficacy of low molecular weight chitosan nanoparticles in antifungal applications. For instance, CNPs under 400 nm suppressed tomato wilt caused by *Fusarium oxysporum f. sp. lycopersici*, leading to improved crop yield [33]. Similarly, field trials by [34] reported significant control of Fusarium Head Blight (FHB) in wheat using CNPs. The findings of this study affirm the potential of nanoscale CNPs (~100 nm) for broad-spectrum antifungal activity, suggesting future exploration across various crop-pathogen systems.

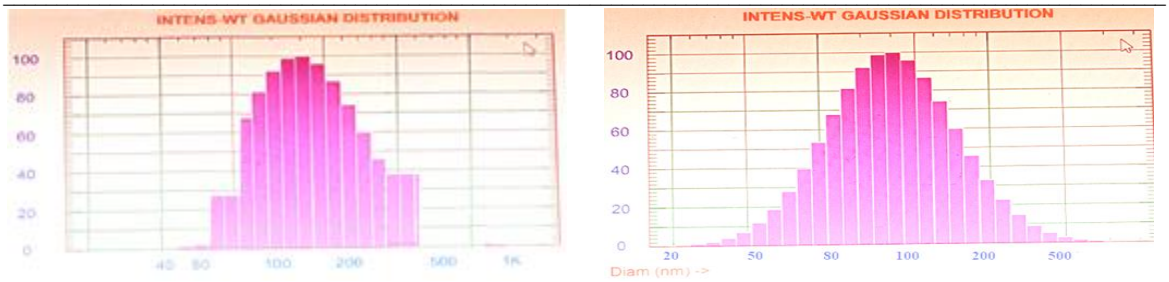

Fig. 2. DLS characters of CNPs loaded with (a) cumin essential oil (b) guava leaves extracts.

3.1.3. Zeta Potential

Zeta potential is a critical indicator of nanoparticle stability in suspension, reflecting the surface charge and electrostatic interactions that prevent particle aggregation. High absolute zeta potential values, whether positive or negative, typically enhance colloidal stability by increasing repulsive forces [35] and [36].

In this study, **guava leaf-loaded CNPs** exhibited a **zeta potential of −15.51 mV** (Figure 3b), indicating moderate stability. The negative charge likely arises from hydroxyl ions present on the nanoparticle surface due to phytochemical capping agents from guava extract. These findings align with previously reported values of −28 mV and −37 mV for chitosan nanoparticles [37] and [38].

Conversely, **cumin oil-loaded CNPs** demonstrated a **positive zeta potential of +29.1 mV** (Figure 3a), attributed to the protonated amine groups in chitosan. Comparable studies reported zeta potentials in the range of +10.58 to +44.23 mV for chitosan-based essential oil nanocapsules [39] and [40]. Essential oils can significantly affect nanoparticle charge; for example, increasing concentrations of Summer savory oil reduced the zeta potential of CNPs from −7.54 to −21.12 mV [41]. Similarly, turmeric EO-loaded chitosan capsules showed values around −21.8 to −23.1 mV [42], emphasizing the impact of oil composition on nanoparticle stability and behavior.

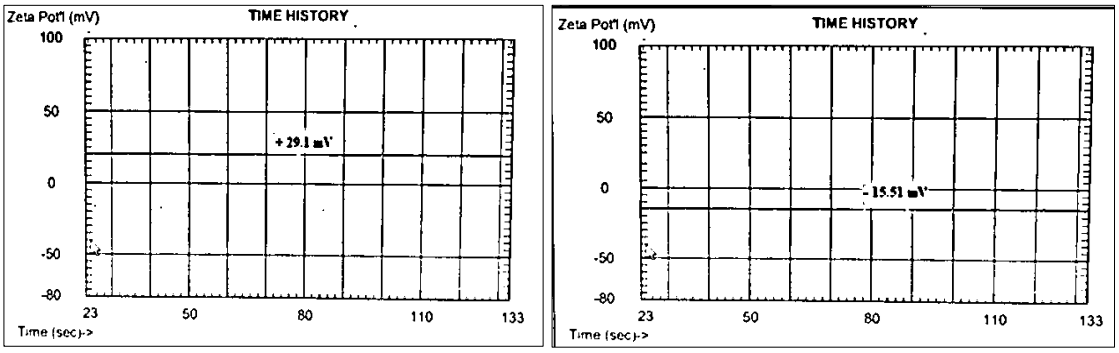

Fig. 3. Zeta potantial characters of CNPs loaded on (a) cumin essential oil (b) guava leaves extracts

3.1.4. X-ray Diffraction (XRD) Analysis

XRD analysis was conducted to evaluate the crystalline structure of cumin oil- and guava extract-loaded CNPs (Figure 4). Both formulations showed a prominent diffraction peak at **2θ = 28°**, confirming the successful encapsulation of bioactive compounds.

Pure CNPs exhibited crystalline peaks at **2θ = 10.06°** (form I) and **20.09°** (form II), indicating a semi-crystalline nature [43]. Upon loading with guava extract, peak sharpness declined and broadening occurred, suggesting reduced crystallinity. This structural change is likely due to cross-linking between chitosan and polyphenolic compounds, resulting in imperfect crystal formation [44] and Deepika et al., 2021).

Similarly, the encapsulation of essential oils, such as **Laurus nobilis**, has been reported to reduce peak intensity and broaden XRD profiles, supporting the disruption of chitosan's crystal lattice upon oil integration [45]. These modifications confirm the effective encapsulation of bioactives and structural alterations in the chitosan matrix.

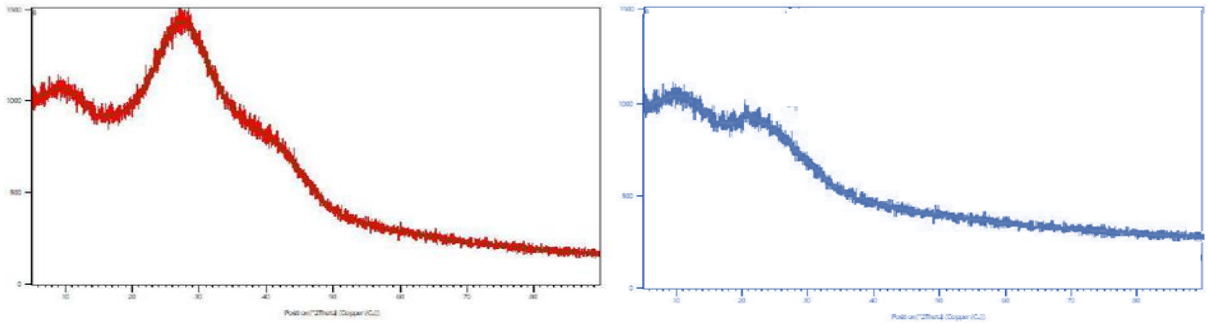

(a) (b)

Fig. 4. XRD characters of CNPs loaded on (a) cumin essential oil (b) guava leaves extracts.

3.1.1 Transmission Electron Microscopy (TEM)

TEM analysis (Figure 5) revealed that the chitosan nanoparticles (CNPs) exhibited a spherical morphology, smooth surfaces, and no visible cracks. Both guava extract (GE)-loaded and cumin oil (CO)-loaded CNPs were well dispersed, indicating stability during synthesis. All particles were smaller than 100 nm, consistent with DLS measurements (Figure 3). Variations in size likely stem from differences in synthesis conditions and methods used [46] and [47].

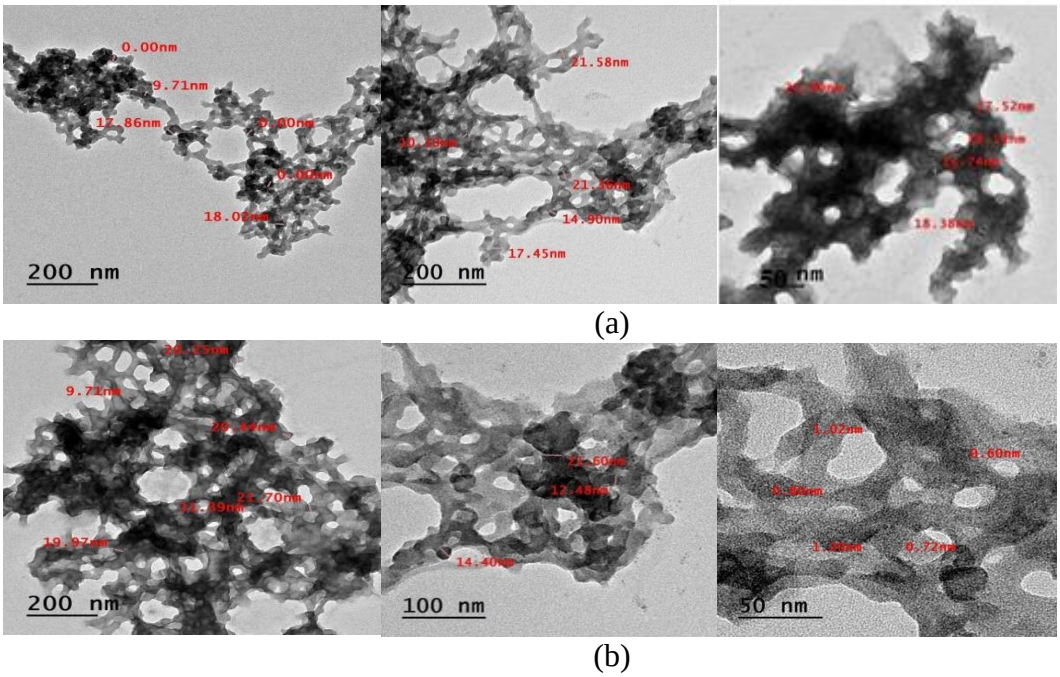

(a)

(b)

Fig. 5. TEM characters of CNPs loaded on (a) cumin essential oil (b) guava leaves extracts

3.2 Antifungal Activity

3.2.1 *In Vitro* Evaluation

The antifungal efficacy of GE- and CO-loaded CNPs against *Fusarium oxysporum* was assessed (Table 1; Figure 6). GE-loaded CNPs showed significantly higher inhibition zones compared to CO-loaded ones, with the highest inhibition at 125

µg/mL (6.7 mm) and 67.5 µg/mL (5.6 mm). The nanoparticles outperformed the synthetic fungicide Rizolex, suggesting their potential as effective biocontrol agents [48].

The inhibitory potential of different concentrations of guava extraction (GE) loaded CNPs and cumin oil (CO) loaded CNPs against *F. oxysporum* growth was presented in Table 3

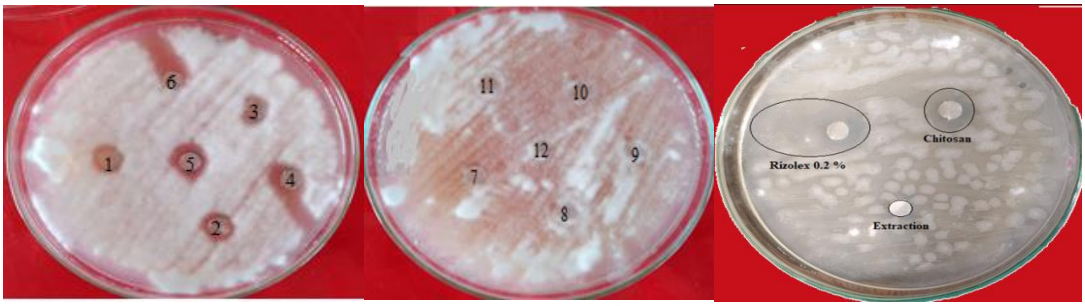

(a) (b) (c)

Fig. 6. (a) Anti-fungal inhibition for nanoparticles obtained from guava extraction 1= 67.5, 2= 125,3=166, 4=250, 5=333 and 6 = 500 ppm; (b) Anti-fungal inhibition for nanoparticles obtained from cumin oil 7= 67.5, 8= 125,9=166, 10=250, 11=333 and 12 = 500 ppm and (c) Rizolex, guava extraction and chitosan.

Table (1) Antifungal activity determination against *F. oxysporum* after exposed to CNPs loaded on guava leaves extract and cumin oil by MIZ (minimum inhibition zone)

CNPs – GE ug/ml	Inhibition zone mm	CNPs - CO	Inhibition zone mm
67.5	5.6 ± 0.23	67.5	1.1±0.10
125	6.7 ± 0.11	125	1.2±0.12
166	4.3 ± 0.31	166	1.0±0.13
250	2.7 ± 0.44	250	1.7±0.11
333	2.8 ± 0.12	333	1.8±0.10
500	2.5 ± 0.26	500	1.6±0.11
Resolix	28.0 ± 0.12	-	-
Chitosan	0.9 ± 0.22	-	-
Guava extraction (GE)	0.0 ± 0.0	-	-
L.S.D 5 %	0.043		0.022

The enhanced efficacy of GE-loaded CNPs could be attributed to their improved penetration and synergistic interactions among active components. Chitosan may also interact with phenolic compounds in GE, contributing to fungal inhibition [49] and [50].

3.2.2 *In Vivo* Evaluation

3.2.2.1 Morphological Response

In pot trials, CNPs at 1500 ppm significantly improved cumin plant growth metrics such as height, number of branches, inflorescences, and biomass (Table 2). This treatment consistently outperformed the positive control and showed comparable or superior results to the synthetic fungicide across two growing seasons.

Table (2) Effect of CNPs loaded on guava leaves extract against *F. oxysporium* fungi on *Cuminum cyminum* morphological shape

	Plant height	Branches number	Inflorescences number	Fresh weight	Dry weight	Percent disease index
Negative control	34.0	8.66	8.33	53.46	23.50	0.00
Positive control	14.0	4.00	4.66	29.33	12.00	95.5
Comparative Fungicide	21.3	5.33	7.00	41.33	18.33	65.8
chitosan NPS 500 ppm	17.0	4.33	4.66	33.66	12.66	55.6
chitosan NPS 1000 ppm	19.3	5.00	6.33	37.33	15.33	63.6
chitosan NPS 1500 ppm	26.0	6.66	7.00	47.33	19.33	71.2
LSD 5 % [season 1]	**4.63**	**1.109**	**1.32**	**3.208**	**1.716**	**2.41**
Negative control	45	13	12.33	55.66	25	0.00
Positive control	18.33	5.33	5.33	31.33	15	92.4
Comparative Fungicide	32.66	10.66	9	45.33	21.33	69.3
chitosan NPS 500 ppm	24.66	7	12.6	35.66	14.66	60.3
chitosan NPS 1000 ppm	28.33	7.66	7.33	41.66	18.33	69.6
chitosan NPS 1500 ppm	37.66	12.33	10.66	48	21	77.2
LSD 5 % [season 2]	**3.820**	**1.677**	**1.185**	**3.137**	**2.408**	**2.03**

The percentage of disease incidence (PDI) was reduced with increasing CNP concentrations. However, while CNPs at 1500 ppm showed improved plant performance, the PDI remained higher than that observed with fungicide treatment, suggesting the need for optimization.

3.2.2.2 Chemical Composition

CNPs application increased the accumulation of total soluble phenols, flavonoids, and total antioxidants in cumin plants under fungal stress (Table 3). CNPs at 1500 ppm enhanced phenol content and antioxidant activity more effectively than lower concentrations but remained slightly lower than fungicide treatment.

Table (3) Effect of CNPs loaded on guava leaves extract against *F. oxysporium* fungi on total phenols, total flavonoids and total antioxidants of *Cuminum cyminum*

	T. phenol	T. Flavonoids	T. Antioxidants
Negative control	0.21	0.054	67.0
Positive control	0.74	0.032	74.9
Comparative Fungicide	0.72	0.043	83.2
chitosan NPS 500 ppm	0.41	0.033	56.3
chitosan NPS 1000 ppm	0.47	0.062	64.8
chitosan NPS 1500 ppm	0.52	0.066	75.0
LSD 5 % [season 1]	**0.036**	**0.023**	**1.03**

Negative control	0.23	0.044	55.0
Positive control	0.88	0.012	82.0
Comparative Fungicide	0.64	0.033	77.3
chitosan NPS 500 ppm	0.52	0.020	44.8
chitosan NPS 1000 ppm	0.55	0.027	45.3
chitosan NPS 1500 ppm	0.68	0.031	53.4
LSD 5 % [season 2]	**0.042**	**0.026**	**1.92**

The plants exposed to fungicide increased phenols to 0.72 mg/100 g fw compared with control (0.21). Increasing concentration of CNPs from 500 ppm to 1500 ppm increased phenols contents gradually to 0.41, 0.47 and 0.52 mg/100 g FW, respectively. At the second season, in all treatments gave increasing in phenols contents compared with the first season. CNPs scored slight increasing 0.52, 0.55 and 0.68 mg/ 100 g fw, respectively. While, infected plants without any treatments (positive control) gave the highest amount of phenols during two seasons (0.88 mg/100 g fw).

In total flavonoid, the first season gave gradually increasing in the plants treated with CNPs which scored 0.033, 0.062 and 0.066 mg/100 g fw, respectively compared with 0.054 for negative control and 0.032 for positive control. These values decreased in the second season for all treatments, CNPs treatments scored 0.020; 0.027 and 0.031 mg/100 g fw. Compared with 0.044; 0.012 and 0.033 mg/100 g fw for negative control; positive control and plant treated with fungicide, respectively.

In total antioxidants, the first season gave gradually increasing in the plants treated with CNPs which scored 56.3, 64.8 and 75 %, respectively compared with 67.0 % for negative control and 74.9 % for positive control. These values decreased in the second season for all treatments, CNPs treatments scored 44.8; 45.3 and 53.4 mg/100 g fw. Compared with 55.0; 82.0 and 77.3 mg/100 g fw for negative control; positive control and plant treated with fungicide, respectively.

GC-MS Analysis of Essential Oil

The chemical profiling of cumin essential oil showed that cumin alcohol and cuminaldehyde were the dominant components as shown in Table 4. The CNPs-GE 1500 treatment yielded the highest concentrations of these compounds (39.93% and 34.42%, respectively), surpassing both untreated and fungicide-treated plants. Lower levels of γ-terpinene and β-pinene were also observed, indicating enhanced oil quality. These results align with previous studies and support the role of chitosan nanoparticles in boosting the biosynthesis of valuable secondary metabolites [51] and [52].

Table (4) Constituents (%) of essential oils for *Cuminum cyminum*

No	R.T.	Components	Components concentration (%)			
			Control (-)	Control (+)	Rezolix ®	CNPs-GE1500
1	6.43	α-Thujene	-	-	0.10	-
2	6.53	α-Pinene	0.86	0.37	0.41	0.18
3	6.71	α-Thujenal	-	-	0.01	-
4	7.07	β-Pinene	12.01	7.47	7.92	4.53
5	7.37	Furan, 2-pentyl-	-	-	0.02	-
6	7.65	α-Phellandrene	1.07	0.77	0.99	0.48
7	7.76	o-Cymene	6.91	8.24	8.24	5.07
8	8.02	4-thujene	0.59	0.55	0.48	0.39
9	8.27	Eucalyptol	-	-	-	0.07
10	8.30	γ-Terpinene	18.55	16.93	14.58	8.32
11	8.84	Menthene	-	-	0.03	-
12	8.91	trans-4-Thujanol	-	-	0.03	-
13	9.08	Nonanal	-	-	0.03	-
14	9.17	Citronellylvalerate	-	-	0.02	-
15	9.29	trans-Sabinenehydrate	-	-	0.06	0.08
16	9.45	3-Carene	-	-	0.04	-
17	9.59	2-p-Menthen-1-ol	-	-	0.02	-
18	9.68	Isopinocarveol	-	-	0.11	-
19	9.74	Pinocarvone	-	-	0.06	-
20	9.84	2-Cyclohexenol	-	-	0.03	0.08
21	9.96	Pulegone	0.06	0.13	0.15	0.72
22	10.19	3-p-Menthen-7-al	2.39	1.09	1.03	-
23	10.37	α-Terpineol	-	-	0.07	0.03

24	10.43	α-Terpinyl acetate	0.04	0.02	-	34.42
25	10.55	Cuminaldehyde	23.71	28.35	28.80	-
26	11.10	Cuminaldehyde	0.09	0.11	0.11	39.77
27	11.19	Cumin alcohol	30.85	33.22	30.67	0.16
28	11.45	Cumin alcohol	0.07	0.10	0.50	-
29	11.81	p-Cymen-7-ol	-	-	0.23	-
30	11.88	Bornyl acetate	-	-	0.22	-
31	12.01	Myrtenyl acetate	-	-	0.06	-
32	12.13	Myrtenyl acetate	-	-	0.14	-
33	12.21	p-Cymen-7-ol	-	-	0.29	-
34	12.36	p-Mentha-1,4-dien-7-ol	0.11	-	-	-
35	12.54	4-Acetyl-3-methylphenol	-	-	0.02	-
36	13.20	2-Caren-10-al	-	-	0.01	-
37	13.24	Copaene	-	-	0.02	0.22
38	13.36	Daucene	0.23	0.26	0.15	0.05
39	13.45	β-Calarene	0.05	0.06	0.04	-
40	13.68	Aromandendrene	-	-	0.01	0.13
41	13.76	Caryophyllene	0.15	0.17	0.13	0.05
42	13.89	trans-α-Bergamotene	0.05	0.06	0.05	-
43	14.13	β-Farnesene	-	-	0.18	1.09
44	14.25	Aromandendrene	0.63	1.27	1.07	0.06
45	14.49	Longifolene	0.06	0.08	0.06	-
46	14.58	α-himachalene	-	-	0.07	0.05
47	14.62	α-himachalene	0.05	0.12	0.05	-
48	15.05	2-Ethyl-5-n-propylphenol	-	-	0.05	-
49	15.17	Tricyclo[4.4.0.0(2.7)]dec-3-ene	-	-	0.06	-
50	15.33	Caryophyllene oxide	-	-	0.24	0.04
51	15.43	Caryophyllene oxide	-	0.05	0.20	0.50
52	15.56	Carotol	0.51	0.57	0.79	-
53	15.72	Longifolene	-	-	0.05	-
54	15.82	Ledene oxide-(II)	-	-	0.05	-
55	15.92	Cedren-13-ol	-	-	0.03	-
56	15.98	Caryophyllene	-	-	0.08	-
57	16.20	7-epi-α-eudesmol	-	-	0.16	-
58	16.28	Isocedrol	-	-	0.04	-
59	16.58	Cyclopropanol, 1-(3,7-dimethyl-1-	-	-	0.23	-
60	17.14	octenyl)-	-	-	0.05	-
61	17.67	p-Methylbenzamide	-	-	0.06	-
62	18.10	7-Hydroxy-2,5,8-quinoline trione	-	-	0.05	-
63	18.38	2-Pentadecanone, 6,10,14-trimethyl-	-	-	0.02	-
64	18.94	Cyclotetradecane	-	-	0.09	-
65	19.55	1,4-Dibutyl benzene-1,4-dicarboxyl	0.64	-	0.14	-
66	20.21	Pendimethalin	-	-	0.08	-
67	20.53	Cyclohexadecane	0.12	-	0.14	-
68	21.33	Caprylic anhydride	0.20	-		
		Buprofezin				
Total identified compounds			100	99.42	99.92	96.49

3.1.1.1. *Cytotoxicity effect of CNPs*

The impact of cumin oil from different treatments on Vero cells across various concentrations was assessed, as presented in Figures 7–10. The tested oils were derived from *Rezolex*®-treated infected plants, non-infected plants (negative control), plants treated with CNPs + GE at 1500 ppm, and untreated infected plants, respectively**.**For cytotoxicity of chitosan nanoparticles of human vero cells with TPP as crosslinker containing inside GE phenolic compounds showed low toxicity at high concentrations (IC_{50} 570.29 ppm) of CNPs + GE 1500 ppm compared with untreated plants (negative control) that scored IC_{50} at 291.46 ppm. On the other hand, cytotoxicity of plants treated with Rezolix ® and infected plants were decreased to 71.9 and 73.8 ppm, respectively. These results explain the cumin oil obtained from plants treated with Rezolix ® and infected plants had negative effect on normal cell activity which decreased to 50 % at low concentrations 71.9 and 73.8 ppm while the same percentage (50%) gave cell activity at 570.29 ppm of CNPs + GE that indicated chitosan nanoparticles was save for human cells compared with artificial fungicide. These results were agreement with those found by [53,54,55,56]who investigated the cytotoxicity of chitosan nanoparticles using Caco-2 cells (human colorectal adenocarcinoma cells) and the MTT-assay. All studies showed good cell viability (>80%) for particles ranging from 126 to 1,000 nm In one of the studies, the cell viability was lower in pH 6 than in pH 7.4. The surface charge was approximately the same, but the particle size was significantly smaller in pH 6 (25 ± 7 nm, 5.3 ± 2.8 mV) than in pH 7.4 (333 ± 43 nm, 3.3 ± 0.4 mV) [54]. The authors suggested that particle size had more influence on the cytotoxicity in Caco-2 cells than the positive surface charge, because of easier cellular uptake of small particles than larger ones [54]. This is in accordance with [53] who showed that chitosan nanoparticles as compared to chitosan molecules accumulated to a higher extent intracellularly, but in

spite of high intracellular concentration of chitosan nanoparticles, the Caco-2 cells showed good viability. Another study reported no difference in cytotoxicity when comparing chitosan nanoparticles of increasing size from 200 to 1,000 nm [57].

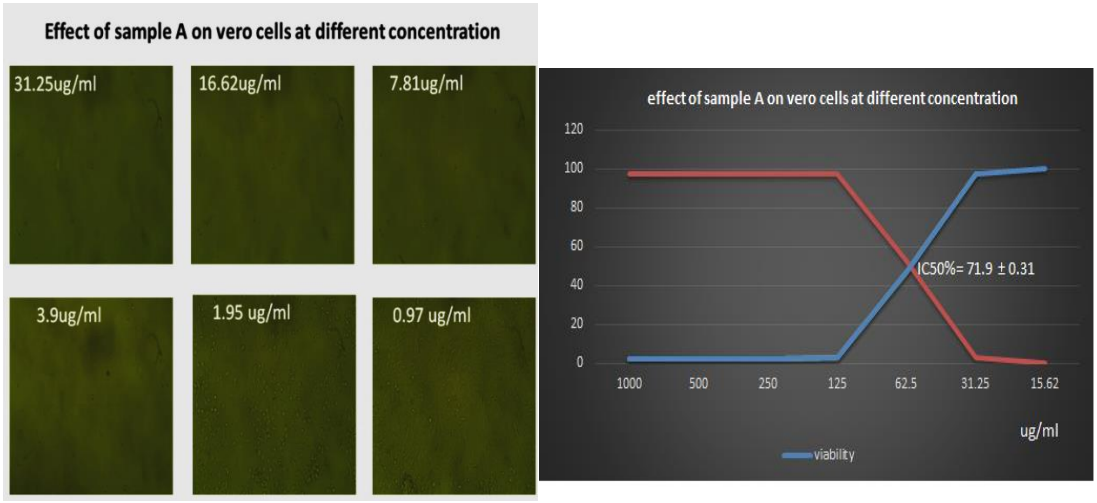

Fig. 7. Effect of cumin oil obtained from Rezolex ® treated infected plants onvero cells at different concentrations

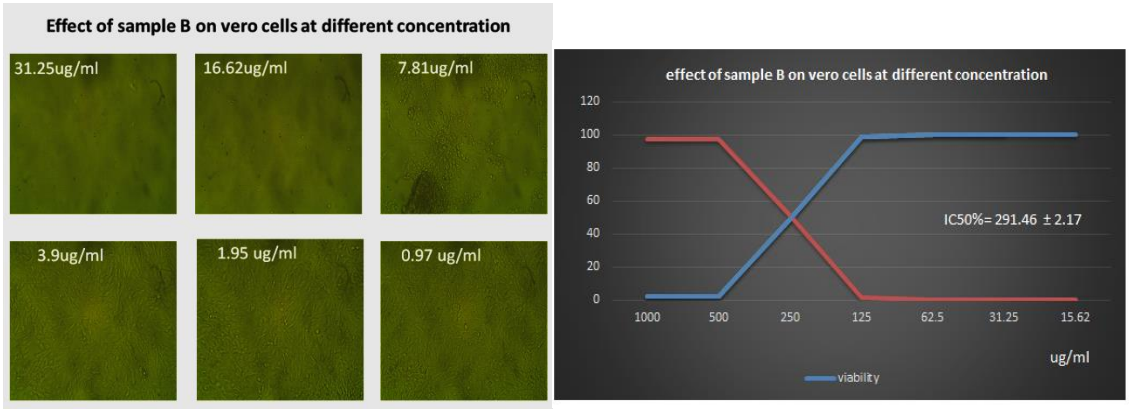

Fig. 8. Effect of oil obtained from non-infected plants (negative control) on vero cells at different concentrations

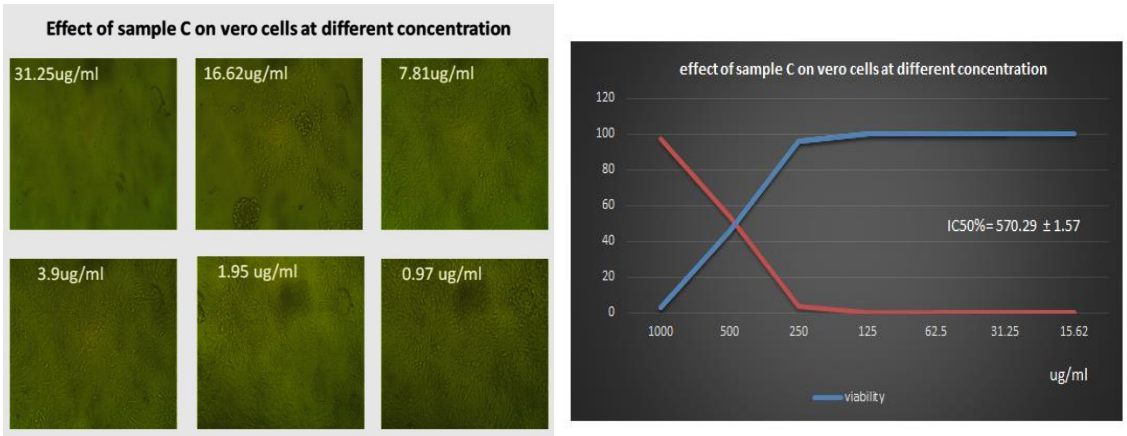

Fig. 9. Effect of oil obtained from CNPs + GE 1500 ppm treated infected plants on vero cells at different concentrations

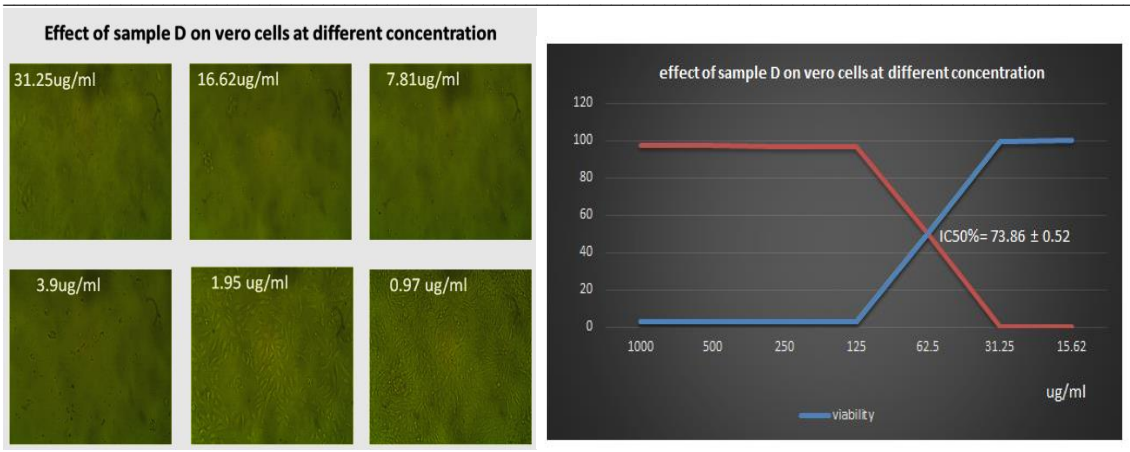

Fig. 10. Effect of oil obtained from un-treated infected plantson vero cells at different concentrations

Also, **[58]** revealed that Chitosan caused complete reduction in growth of *F. oxysporum*the causal of pepper wilt (*Capsicum annum* L.). Similar results were recorded by many investigators with various crops. Chitin and chitosan as well the safe materials were reported to induce resistance by [59]. These findings in general agree with [60] who stated that salicylic acid completely inhibited the mycelial development of *F. oxysporum*f. sp. *lycopersici in vitro.* As well as, clove gave complete inhibitory effect on growth of *F. oxysporum*followed by mint, while, cumin oil showed the lowest inhibitory activity in controlling *F. oxysporum*, these results explain why cumin oil have no effect on F. oxysporium although we used chitosan nano emulsion of CO with chitosan. *F. oxysporium* was more resistant for cumin oil due to cinammaldehyde and cumin alcohol work as a stimulant for mycelium growth.These results are in agreement with **[61]** who reported that the best results were obtained with clove oil and its major component eugenol in controlling *F. oxysporum*f. sp. *lycopersici,* and those of **[62]** who reported that *F. oxysporum*f. sp. *gladioli* was totally inhibited with clove oil

4. Conclusion

The findings indicate that chitosan nanoparticles synthesized with guava leaf extract (CNPs-GE1500) represent the most effective natural antifungal treatment against *Fusarium oxysporum* in cumin. This formulation significantly enhanced plant growth, reduced disease severity, and improved essential oil quality, highlighting its potential as a sustainable alternative to chemical fungicides.

5. Conflicts of interest

There are no conflicts to declare.

6. Formatting of funding sources

No funding sources in a standard way to facilitate compliance to funder's requirements.

7. References and Bibliography

[1] Elchaghaby, M.A., Abd El-Kader, S.F., & Aly, M.M. (2022). Bioactive composition and antibacterial activity of three herbal extracts (lemongrass, sage, and guava leaf) against oral bacteria: An *in vitro* study. *Journal of Oral Biosciences*, 64(1), 114–119. https://doi.org/10.1016/j.job.2022.01.005

[2] Singh, R. P., Gangadharappa, H. V., &Mruthunjaya, K. (2017). *Cuminum cyminum* - A popular spice: An updated review. *Pharmacognosy Journal*, 9(3), 292–301. https://doi.org/10.5530/pj.2017.3.51

[3] El Amraoui, K., Ichir, L.L., &Bakali, A.H. (2024). Physical characterization of cumin (*Cuminum cyminum* L.) schizocarps of different origins cultivated in Morocco. *Journal of the Saudi Society of Agricultural Sciences*, 23(5), 369–383. https://doi.org/10.1016/j.jssas.2024.03.006

[4] Abo-Elyousr, K.A.M., Saad, M.M., Al-Qurashi, A.D., Ibrahim, O.H.M., & Mousa, M.A.A. (2022). Management of cumin wilt caused by *Fusarium oxysporum* using native endophytic bacteria. *Agronomy*, 12(10), 1–14. https://doi.org/10.3390/agronomy12102510

[5] El-Sayed, E.S.R., Mohamed, S.S., Mousa, S.A., El-Seoud, M.A.A., Elmehlawy, A.A., &Abdou, D.A. (2023). Bifunctional role of some biogenic nanoparticles in controlling wilt disease and promoting growth of common bean. *AMB Express*, 13(1), 11. https://doi.org/10.1186/s13568-023-01546-7

[6] Gomaa, N. A., Mahdy, A. M., Fawzy, R. N., & Ahmed, G. A. (2021). Green synthesis of silver nanoparticles by plant extracts to control tomato wilt disease caused by *Fusarium oxysporum* f. sp. *lycopersici*. *International Journal of Sustainable Development and Science*, 4(3), 1–14. https://doi.org/10.21608/ijsrsd.2021.211253

[7] Kumawat, G. L., et al. (2022). Screening of cumin (*Cuminum cyminum* L.) germplasm to blight and wilt diseases caused by *Alternariaburnsii* and *Fusarium oxysporum* f. sp. *cumini*. *Biological Forum – An International Journal*, 14(1), 1412–1415.

[8] Karunarathna, A., Wijeratne, D., Zhang, X., & Hyde, K. D. (2023). An examination of how climate change could affect the future spread of *Fusarium* spp. around the world using correlative models to model the changes. *Journal of Fungi*, *9*(4), 398. https://doi.org/10.3390/jof9040398

[9] Dharajiya, D.T., Shukla, N., Pandya, M., Joshi, M., Patel, A.K., & Joshi, C.G. (2023). Resistant cumin cultivar GC-4 counters *Fusarium oxysporum* f. sp. *cumini* infection through upregulation of steroid biosynthesis, limonene and pinene degradation, and butanoate metabolism pathways. *Frontiers in Plant Science*, 14, 1204828. https://doi.org/10.3389/fpls.2023.1204828

[10] Hassan, M. A., El-Saadony, M. T., Mostafa, N. G., El-Tahan, A. M., Mesiha, P. K., El-Saadony, F. M., Hassan, A. M., El-Shehawi, A. M., & Ashry, N. M. (2021). The use of previous crops as sustainable and eco-friendly management to fight *Fusarium oxysporum* in sesame plants. *Saudi Journal of Biological Sciences*, 28(10), 5849–5859. https://doi.org/10.1016/j.sjbs.2021.06.041

[11] El-Abeid, S.E., Mosa, M.A., El-Tabakh, M.A., Saleh, A.M., El-Khateeb, M.A., &Haridy, M.S. (2023). Antifungal activity of copper oxide nanoparticles derived from *Zizyphus spina* leaf extract against *Fusarium* root rot disease in tomato plants. *Journal of Nanobiotechnology*, 22(1), 1–24. https://doi.org/10.1186/s12951-023-02281-8

[12] Abubakar, A., Ahmad, K., Siddique, Y., Wahab, M.A.A., Kutawa, A.B., Abdullahi, A., Zobir, S.A.M., Abdu, A., & Abdullah, S.N.A. (2023). *Fusarium* wilt of banana: Current update and sustainable disease management. *Horticultural Plant Journal*, 9(1), 1–28. https://doi.org/10.1016/j.hpj.2022.02.004

[13] Wang, Y., Hao, D., Jiang, H., Fei, Z., Zhao, R., Gao, J., Li, G., & Wang, C. (2025). Identification and fungicide sensitivity of *Fusarium oxysporum*, the cause of Fusarium wilt on *Codonopsispilosula* in Shanxi Province (Lu Dangshen), China. *Crop Protection*, 190, 107083. https://doi.org/10.1016/j.cropro.2024.107083

[14] Parada, J., Tortella, G., Seabra, A. B., Fincheira, P., &Rubilar, O. (2024). Potential antifungal effect of copper oxide nanoparticles combined with fungicides against *Botrytis cinerea* and *Fusarium oxysporum*. *Antibiotics*, 13(2), 11.

[15] Sun, Y., Wang, Y., Han, L. R., Zhang, X., & Feng, J. T. (2017). Antifungal activity and action mode of cuminic acid from the seeds of *Cuminum cyminum* L. against *Fusarium oxysporum* f. sp. *niveum* (FON) causing Fusarium wilt on watermelon. *Molecules*, 22(12), 2053. https://doi.org/10.3390/molecules22122053

[16] Extracts, P., et al. (2018). Investigation of potential biological control of *Fusarium oxysporum* f. sp. *in vitro*. *Fungal Genomics & Biology*, 8(1), 8–11. https://doi.org/10.4172/2165-8056.1000155

[17] Abdelaziz, A.M., Salem, S.S., Khalil, A.M.A., El-Wakil, D.A., Fouda, H.M., & Hashem, A.H. (2022). Potential of biosynthesized zinc oxide nanoparticles to control *Fusarium* wilt disease in eggplant (*Solanum melongena*) and promote plant growth. *BioMetals*, 35(3), 601–616. https://doi.org/10.1007/s10534-022-00391-8

[18] González-Merino, A. M., Hernández-Juárez, A., Betancourt-Galindo, R., Ochoa-Fuentes, Y. M., Valdez-Aguilar, L. A., & Limón-Corona, M. L. (2021). Antifungal activity of zinc oxide nanoparticles in *Fusarium oxysporum*–*Solanum lycopersicum*pathosystem under controlled conditions. *Journal of Phytopathology*, 169(9), 533–544. https://doi.org/10.1111/jph.13023

[19] Karamian, R., &Kamalnejade, J. (2019). Green synthesis of silver nanoparticles using aqueous seed extract of *Cuminum cyminum* L. and evaluation of their biological activities. *Journal of Nanostructures*, 9(1), 128–141. https://doi.org/10.29252/sjimu.26.5.128

[20] Putri, S. E., Ahmad, A., Raya, I., Tjahjanto, R. T., &Irfandi, R. (2023). Synthesis and antibacterial activity of chitosan nanoparticles from black tiger shrimp shells (*Penaeus monodon*). *Egyptian Journal of Chemistry*, 66(8), 129–139. https://doi.org/10.21608/ejchem.2022.148340.6417

[21] Talab, A. S., Hussein, A., Kamil, M. M., Mostafa, S., Hegazy, N. A., & Mahmoud, K. F. (2024). Synthesis and characterization of chitosan nanoparticles from some crustacean wastes. *Egyptian Journal of Chemistry*, 67(5), 23–42. https://doi.org/10.21608/ejchem.2023.228113.8401

[22] Singleton, V. L., Orthofer, R., &Lamuela-Raventós, R. M. (1999). Analysis of total phenols and other oxidation substrates and antioxidants by means of Folin-Ciocalteu reagent. *Methods in Enzymology*, 299, 152–178. https://doi.org/10.1016/S0076-6879(99)99017-1

[23] Woisky, R., & Salatino, A. (1998). Analysis of propolis: Some parameters and procedures for chemical quality control. *Journal of Apicultural Research*, 37, 99–105.

[24] Brand-Williams, W., Cuvelier, M.E., & Berset, C. (1995). Use of a free radical method to evaluate antioxidant activity. *Lebensmittel-Wissenschaft und -Technologie*, 28(1), 25–30.

[25] Clevenger, J.F. (1928). Apparatus for the determination of volatile oil. *Journal of the American Pharmaceutical Association*, 17(4), 345–349.

[26] Stenhagen, E., Abrahamsson, S., & McLafferty, F. W. (1974). *Registry of mass spectral data* (12th ed.). Wiley & Sons.

[27] Jennings, W., &Shibamoto, T. (1980). *Qualitative analysis of flavor and fragrance volatiles by glass capillary gas chromatography* (1st ed.). Academic Press.

[28] Karakaş, D., Ari, F., & Ulukaya, E. (2017). The MTT viability assay yields strikingly false-positive viabilities although the cells are killed by some plant extracts. *Turkish Journal of Biology*, *41*(6), 919-925.
[29] Alley, M.C., Scudiero, D.A., Monks, A., Hursey, M.L., Czerwinski, M.J., Fine, D.L., Abbott, B.J., Mayo, J.G., Shoemaker, R.H., & Boyd, M.R. (1988). Feasibility of drug screening with panels of human tumor cell lines using a microculture tetrazolium assay. *Cancer Research*, 48(3), 589–601.
[30] Maxwell, S. E., & Delaney, H. D. (1990). *Designing experiments and analyzing data: A model comparison perspective*. Wadsworth.
[31] Saharan, V., Mehrotra, A., Khatik, R., Rawal, P., Sharma, S. S., & Pal, A. (2013). Synthesis of chitosan-based nanoparticles and their *in vitro* evaluation against phytopathogenic fungi. *International Journal of Biological Macromolecules*, 62, 677–683.
[32] Dananjaya, S.H.S., Erandani, W.K.C.U., Kim, C.H., Nikapitiya, C., Lee, J., & De Zoysa, M. (2017). Comparative study on antifungal activities of chitosan nanoparticles and chitosan-silver nanocomposites against *Fusarium oxysporum* species complex. *International Journal of Biological Macromolecules*, 105, 478–488.
[33] Sathiyabama, M., & Charles, R. E. (2015). Fungal cell wall polymer-based nanoparticles in protection of tomato plants from wilt disease caused by *Fusarium oxysporum* f. sp. *lycopersici*. *Carbohydrate Polymers*, 133, 400–407. https://doi.org/10.1016/j.carbpol.2015.06.103
[34] Kheiri, A., Jorf, S. M., Malihipour, A., Saremi, H., &Nikkhah, M. (2017). Synthesis and characterization of chitosan nanoparticles and their effect on *Fusarium* head blight and oxidative activity in wheat. *International Journal of Biological Macromolecules*, 102, 526–538.
[35] Gumustas, M., Sengel-Turk, C. T., Gumustas, A., Ozkan, S. A., & Uslu, B. (2017). Effect of polymer-based nanoparticles on the assay of antimicrobial drug delivery systems. In *Multifunctional Systems for Combined Delivery, Biosensing and Diagnostics* (pp. 67–108). Elsevier.
[36] Lu, G. W., & Gao, P. (2010). Emulsions and microemulsions for topical and transdermal drug delivery. In *Handbook of Non-Invasive Drug Delivery Systems* (pp. 59–94). William Andrew Publishing.
[37] Sathiyabama, M., & Parthasarathy, R. (2016). Biological preparation of chitosan nanoparticles and its*in vitro* antifungal efficacy against some phytopathogenic fungi. *Carbohydrate Polymers*, 151, 321–325.
[38] Manikandan, A., & Sathiyabama, M. (2016). Preparation of chitosan nanoparticles and its effect on detached rice leaves infected with *Pyriculariagrisea*. *International Journal of Biological Macromolecules*, 84, 58–61.
[39] Hasani, S., Ojagh, S. M., & Ghorbani, M. (2018). Nanoencapsulation of lemon essential oil in chitosan-Hicap system. Part 1: Study on its physical and structural characteristics. *International Journal of Biological Macromolecules*, 115, 143–151.
[40] Matshetshe, K. I., Parani, S., Manki, S. M., & Oluwafemi, O. S. (2018). Preparation, characterization and *in vitro* release study of β-cyclodextrin/chitosan nanoparticles loaded *Cinnamomum zeylanicum* essential oil. *International Journal of Biological Macromolecules*, 118(Part A), 676–682.
[41] Feyzioglu, G. C., &Tornuk, F. (2016). Development of chitosan nanoparticles loaded with summer savory (*Saturejahortensis* L.) essential oil for antimicrobial and antioxidant delivery applications. *LWT - Food Science and Technology*, 70, 104–110.
[42] Lertsutthiwong, P., Rojsitthisak, P., &Nimmannit, U. (2009). Preparation of turmeric oil-loaded chitosan-alginate biopolymericnanocapsules. *Materials Science and Engineering: C*, 29(3), 856–860.
[43] Pastor, C., Sánchez-González, L., Chiralt, A., Cháfer, M., & González-Martínez, C. (2013). Physical and antioxidant properties of chitosan and methylcellulose-based films containing resveratrol. *Food Hydrocolloids*, 30(1), 272–280.
[44] Ji, J., Hao, S., Wu, D., Huang, R., & Xu, Y. (2011). Preparation, characterization and *in vitro* release of chitosan nanoparticles loaded with gentamicin and salicylic acid. *Carbohydrate Polymers*, 85(4), 803–808.
[45] Cai, J., Yang, D., & Wang, Q. (2023). Preparation and characterization of chitosan nanoparticles loaded with *Athyriumsinense* essential oil with antibacterial properties against *Pectobacteriumcarotovorum* subsp. *carotovorum*. *Industrial Crops and Products*, 195, 116382.
[46] Kavaz, D., Idris, M., & Onyebuchi, C. (2019). Physicochemical characterization, antioxidative, anticancer cell proliferation and antibacterial activity of chitosan nanoparticles loaded with *Cyperusarticulatus* rhizome essential oils. *International Journal of Biological Macromolecules*, 123, 837–845.
[47] Zhao, C. X., He, L., Qiao, S. Z., &Middelberg, A. P. (2011). Nanoparticle synthesis in microreactors. *Chemical Engineering Science*, 66(7), 1463–1479.
[48] Prakash, S., Chakrabarty, T., Singh, A. K., & Shahi, V. K. (2012). Silver nanoparticles built-in chitosan modified glassy carbon electrode for anodic stripping analysis of As(III) and its removal from water. *ElectrochimicaActa*, 72, 157–164.
[49] Juarez-Morales, L. A., Hernandez-Cocoletzi, H., Chigo-Anota, E., Aguila-Almanza, E., &Tenorio-Arvide, M. G. (2017). Chitosan–aflatoxins B1, M1 interaction: A computational approach. *Current Organic Chemistry*, 21(28), 2877–2883.
[50] Menazea, A. A. (2020). Femtosecond laser ablation-assisted synthesis of silver nanoparticles in organic and inorganic liquids medium and their antibacterial efficiency. *Radiation Physics and Chemistry*, 168, 108616.
[51] Mahdi, A., Ibrahim, H. M., Farroh, K., Saleh, E., & Ghaly, O. (2021). Chitosan nanoparticles and its impact on growth, yield, some biochemical and molecular markers in *Silybiummarianum*. *Egyptian Journal of Desert Research*, 71(2), 163–190.

[52] Mahdi, A.A., Suliman, M.N., Farroh, K.Y., Ghaly, O., Hamed, E.S. and Ibrahim, H.M. (2022). Chitosan and amino acids-coated nanoparticles positively altered atropine accumulation, the gene expression of tropinone reductase 1 and the yield of Datura innoxia Mill. *Plant Cell Biotechnology and Molecular Biology*, 23(37–38): 26–50.

[53] Zheng, A.-p., Liu, H.-x., Yuan, L., Meng, M., Wang, J.-c., Zhang, X., et al. (2011). Comprehensive Studies on the Interactions between Chitosan Nanoparticles and Some Live Cells. Journal of Nanoparticle Research. 13 (10), 4765–4776.

[54] Loh, J.W., Yeoh, G., Saunders, M., and Lim, L. Y. (2010). Uptake and Cytotoxicity of Chitosan Nanoparticles in Human Liver Cells. Toxicology and Applied Pharmacolog. 249 (2), 148–157.

[55] Jain, A., Jain, S., Jain, R., and Kohli, D. V. (2015). Coated Chitosan Nanoparticles Encapsulating Caspase 3 Activator for Effective Treatment of Colorectral Cancer. Drug Delivery and Translational Research. 5 (6), 596–610.

[56] Je, H. J., Kim, E. S., Lee, J. S., and Lee, H. G. (2017). Release Properties and Cellular Uptake in Caco-2 Cells of Size-Controlled Chitosan Nanoparticles. Journal of Agricultural and Food Chemistry. 65 (50), 10899–10906.

[57] Abd-El-Kareem, F. 2002. Integrated treatments between bioagents and chitosan on root rot diseases of pea plants under field conditions. Egyptian Journal of Applied Sciences, 17: 257-279.

[58] Ragab, Mona M.M., Ashour, A.M.A., Abdel-Kader, M. M., El-Mohamady, R. and Abdel-Aziz, A. 2012. In vitro evaluation of some fungicides alternatives against Fusarium oxysporum the causal of wilt disease of pepper (Capsicum annum L.). International Journal of Agriculture and Forestry, 2(2):70-77.

[59] Özgönen, H.; Biçici, M. and Erkiliç A. 2001. The effect of salicylic acid and endomycorrhizal fungus Glomus etunicatum on plant development of tomatoes and Fusarium wilt caused by Fusarium oxysporum f. sp. lycopersici. Turkish Journal of Agriculture and Forestry, 25:25-29.

[60] Torre, A.L.; Caradonia, F.; Matere, A. and Battaglia, V. 2016. Using plant essential oils to control Fusarium wilt in tomato plants. European Journal of Plant Pathology, 144: 487-496.

[61] Barrerea-Necha, L.L.; Garduño-Pizaña, C. and Garcia-Barrera, L.J. 2009. In vitro antifungal activity of essential oils and their compounds on mycelial growth of F. oxysporum f. sp. gladioli. Plant Pathology Journal, 8(1):17–21.

[62] Barrerea-Necha, L. L., Garduño-Pizaña, C., & Garcia-Barrera, L. J. (2009). In vitro antifungal activity of essential oils and their compounds on mycelial growth of F. oxysporum f. sp. gladioli. Plant Pathology Journal, 8(1), 17-21.